

The spatial Wilson loops, string breaking, and AdS/QCD

Oleg Andreev*

*Arnold Sommerfeld Center for Theoretical Physics,
LMU-München, Theresienstrasse 37, 80333 München, Germany*

We consider the phenomenon of string breaking in the context of the spatial Wilson loops using the gauge/string duality. In particular, we discuss the impact of light flavors on the pseudopotential. We also introduce the notion of the spatial string breaking distance and estimate it for $SU(3)$ gauge theory in the temperature range $0 - 3T_c$.

I. INTRODUCTION

It is well-known that QCD at high temperature undergoes a phase transition from a confined phase to a deconfined phase.¹ While basic thermodynamical observables show a drastic qualitative change at the transition point, there are some whose structure does not change qualitatively across T_c . One example is the pseudopotential V extracted from spatial Wilson loops. For a rectangular loop \mathcal{C} of length ℓ and width Y along two spatial directions, it is defined as

$$\langle W(\mathcal{C}) \rangle \sim e^{-V(\ell)Y}, \quad \text{as} \quad Y \rightarrow \infty. \quad (1.1)$$

Importantly, at any temperature the spatial Wilson loops obey an area law (for large ℓ and Y), so that $V = \sigma_s \ell$, where σ_s is the spatial string tension [2]. This implies the confinement of magnetic modes.

For temperatures below and just above T_c , the computation of the pseudopotential is strongly influenced by nonperturbative effects and therefore cannot be performed within perturbative QCD. Although lattice gauge theory is one of the basic tools for studying nonperturbative phenomena and has made significant progress in calculating the spatial Wilson loops in four dimensions [3], the need to understand the physics behind computational complexity motivates the use of effective field and string models. A special class of string models, known as AdS/QCD (holographic) models, has attracted much attention in the recent years. The hope is that the gauge/string duality provides new theoretical tools for studying strongly coupled gauge theories.²

This Letter extends our study of the pseudopotentials in pure gauge theories [5] to theories with two light quarks. The phenomenon of string breaking plays a pivotal role in this, as it modifies the large- ℓ behavior of the pseudopotential.

II. KEY FEATURES OF A FIVE-DIMENSIONAL FRAMEWORK

In the context of AdS/CFT (QCD), the discussion of a Wilson loop proceeds as follows. First, one chooses a contour \mathcal{C} on a four-manifold which is the boundary of a five-dimensional manifold. One then considers fundamental strings on this manifold such that the string worldsheet has \mathcal{C} as its boundary. The expectation value of the Wilson loop is schematically given by the worldsheet path integral

$$\langle W(\mathcal{C}) \rangle = \int DX e^{-S_w}, \quad (2.1)$$

where X denotes a set of worldsheet fields and S_w is a worldsheet action. In principle, this integral can be evaluated semiclassically in terms of minimal surfaces satisfying the boundary conditions. The result takes the form

$$\langle W(\mathcal{C}) \rangle = \sum_n w_n e^{-S_n}, \quad (2.2)$$

*Also on leave from L.D. Landau Institute for Theoretical Physics

¹ For 2 + 1 flavor QCD with physical quark masses, this transition is likely a rapid crossover. See, for example, [1].

² For the further development of these ideas in the context of QCD, see the book [4] and references therein.

where S_n represents a regularized minimal area whose relative weight is w_n .³

To illustrate these ideas, we now consider a specific model. This model is well motivated for two reasons: first, it provides the estimates for Wilson loops which agree well with lattice calculations and QCD phenomenology in four dimensions [5–7]; second, its simplicity enables many analytical estimates.

Following [5], we consider a five-dimensional metric which is a simple one-parameter deformation of the Schwarzschild black hole in Euclidean AdS₅. Light quarks are modeled by turning on a scalar field T [8], which accounts for quarks at the string endpoints. Thus, the background takes the form

$$ds^2 = e^{sr^2} \frac{R^2}{r^2} \left(f(r) dt^2 + d\vec{x}^2 + f^{-1}(r) dr^2 \right), \quad T = T(r). \quad (2.3)$$

Here $f(r) = 1 - \frac{r^4}{r_h^4}$ and s is the deformation parameter. The boundary is located at $r = 0$. The Hawking temperature, which is identified with the temperature of the dual gauge theory, is $T = \frac{1}{\pi r_h}$. The critical temperature is determined from the spatial string tension [5]. Explicitly,

$$T_c = \frac{\sqrt{s}}{\pi}. \quad (2.4)$$

To construct string configurations in this background, we need two key ingredients. The first is a Nambu-Goto string governed by the action

$$S_{\text{NG}} = \frac{1}{2\pi\alpha'} \int d^2\xi \sqrt{\gamma^{(2)}}, \quad (2.5)$$

where γ is an induced metric, α' is a string parameter, and ξ^i are worldsheet coordinates. The second is a boundary term

$$S_{\text{q}} = \int d\tau e T, \quad (2.6)$$

which is the usual sigma-model action for strings in a tachyon background. The integral is over a worldsheet boundary, parameterized by τ , and e is a boundary metric.

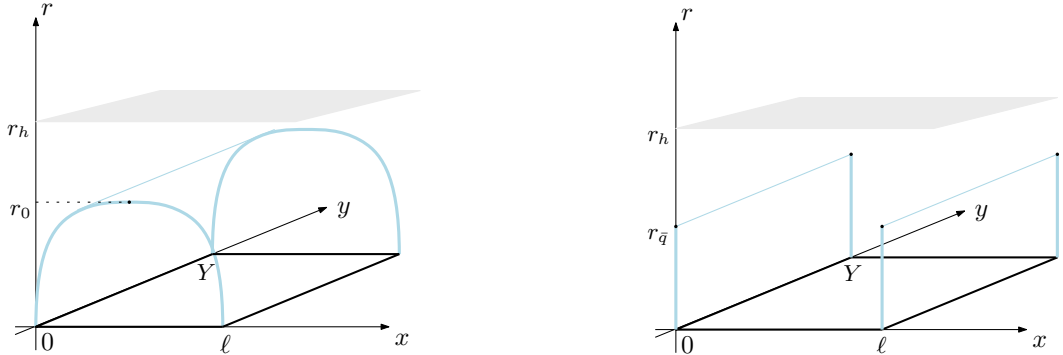


FIG. 1: String configurations in five dimensions. The rectangle at $r = 0$ is shown in bold and the horizon at $r = r_h$ in gray. The string profiles are sketched at $y = 0$ and $y = Y$. Left: A connected configuration. Here r_0 is the r -coordinate of the string turning point. Right: A disconnected configuration. Here $r_{\bar{q}}$ denotes a r -coordinate of the light quarks.

³ The key point is that these areas are divergent, but the divergences are proportional to the circumference of \mathcal{C} .

III. THE PSEUDOPOTENTIAL

Now we want to compute the pseudopotential in the presence of light dynamical quarks. Since V coincides with the heavy quark-antiquark potential at zero temperature, it is natural to consider not only the connected string configuration but also the disconnected one [9]. The latter can be interpreted as a pair of heavy-light mesons created by the formation of a virtual quark-antiquark pair. Both configurations are shown in Fig.1.⁴

A. The connected configuration

The pseudopotential related to the connected configuration can be computed along the lines described in [11]. In the limit $Y \rightarrow \infty$, the area swept out by the string is obtained by parallel transporting it along the y -direction (see Fig.1), yielding the pseudopotential $V_{\text{con}} = S_{\text{NG}}/Y$. An important point is that the side areas at $y = 0$ and $y = Y$ become irrelevant in this limit. For the geometry (2.3), the result is expressed parametrically [5]

$$\begin{aligned} \ell &= 2\sqrt{\frac{\lambda}{s}} \int_0^1 dv v^2 e^{\lambda(1-v^2)} \left(1 - \lambda^2 v^4 \frac{T^4}{T_c^4}\right)^{-\frac{1}{2}} \left(1 - v^4 e^{2\lambda(1-v^2)}\right)^{-\frac{1}{2}}, \\ V_{\text{con}} &= 2g\sqrt{\frac{s}{\lambda}} \int_0^1 \frac{dv}{v^2} \left[e^{\lambda v^2} \left(1 - \lambda^2 v^4 \frac{T^4}{T_c^4}\right)^{-\frac{1}{2}} \left(1 - v^4 e^{2\lambda(1-v^2)}\right)^{-\frac{1}{2}} - 1 - v^2 \right] + 2c. \end{aligned} \quad (3.1)$$

Here c is a normalization constant arising from the renormalization of a linear divergence. The parameter λ is defined as $\lambda = sr_0^2$. It varies from 0 to 1 for $T \leq T_c$ and from 0 to $\frac{T_c^2}{T^2}$ for $T \geq T_c$. This reflects the underlying two-wall pattern, as explained in [5].⁵ The first wall is a soft wall at $r = 1/\sqrt{s}$, which confines the string to the near-boundary region for $T < T_c$, while the second is the horizon, which confines it for $T > T_c$. The walls coincide at $T = T_c$. This pattern qualitatively explains the temperature dependence of the spatial string tension which is temperature-independent below T_c and manifestly dependent above T_c .⁶ In the current model, the spatial string tension is given by

$$\sigma_s = \begin{cases} \sigma & \text{if } T \leq T_c, \\ \sigma \frac{T^2}{T_c^2} \exp\left\{\frac{T_c^2}{T^2} - 1\right\} & \text{if } T \geq T_c, \end{cases} \quad (3.2)$$

where $\sigma = ges$ is the physical string tension at zero temperature [13].

For our purposes here, we need to know the subleading term in the large- ℓ expansion of the pseudopotential. To find it, consider the difference

$$\begin{aligned} V_{\text{con}} - \sigma_s \ell &= 2g\sqrt{s} \left(\frac{1}{\sqrt{\lambda}} \int_0^1 \frac{dv}{v^2} \left[e^{\lambda v^2} \left(1 - \lambda^2 v^4 \frac{T^4}{T_c^4}\right)^{-\frac{1}{2}} \left(1 - v^4 e^{2\lambda(1-v^2)}\right)^{-\frac{1}{2}} - 1 - v^2 \right] \right. \\ &\quad \left. - \sqrt{\lambda} \int_0^1 dv v^2 e^{1+\lambda(1-v^2)} \left(1 - \lambda^2 v^4 \frac{T^4}{T_c^4}\right)^{-\frac{1}{2}} \left(1 - v^4 e^{2\lambda(1-v^2)}\right)^{-\frac{1}{2}} \right) + 2c, \end{aligned} \quad (3.3)$$

where $T < T_c$. Taking the limit $\lambda \rightarrow 1$ yields

$$V_{\text{con}} - \sigma_s \ell = 2g\sqrt{s} \int_0^1 \frac{dv}{v^2} \left[e^{v^2} \left(1 - v^4 \frac{T^4}{T_c^4}\right)^{-\frac{1}{2}} \left(1 - v^4 e^{2(1-v^2)}\right)^{\frac{1}{2}} - 1 - v^2 \right] + 2c. \quad (3.4)$$

Similarly, for $T > T_c$, the difference can be written as

⁴ For computing the ground state pseudopotential, there is no need to involve excited strings, which lead to hybrid pseudopotentials. See, for example, [10].

⁵ A similar pattern persists in the anisotropic case [12].

⁶ We call such behavior "specific" even if it exhibits weak temperature dependence below T_c .

$$V_{\text{con}} - \sigma_s \ell = 2g\sqrt{s} \left(\frac{1}{\sqrt{\lambda}} \int_0^1 \frac{dv}{v^2} \left[e^{\lambda v^2} \left(1 - \lambda^2 v^4 \frac{T^4}{T_c^4} \right)^{-\frac{1}{2}} \left(1 - v^4 e^{2\lambda(1-v^2)} \right)^{-\frac{1}{2}} - 1 - v^2 \right] \right. \\ \left. - \sqrt{\lambda} \frac{T^2}{T_c^2} e^{\frac{T_c^2}{T^2}} \int_0^1 dv v^2 e^{\lambda(1-v^2)} \left(1 - \lambda^2 v^4 \frac{T^4}{T_c^4} \right)^{-\frac{1}{2}} \left(1 - v^4 e^{2\lambda(1-v^2)} \right)^{-\frac{1}{2}} \right) + 2c. \quad (3.5)$$

Taking the limit $\lambda \rightarrow \frac{T_c^2}{T^2}$ then gives

$$V_{\text{con}} - \sigma_s \ell = 2g\sqrt{s} \frac{T}{T_c} \int_0^1 \frac{dv}{v^2} \left[e^{\frac{T_c^2}{T^2} v^2} (1 - v^4)^{-\frac{1}{2}} \left(1 - v^4 e^{2\frac{T_c^2}{T^2}(1-v^2)} \right)^{\frac{1}{2}} - 1 - v^2 \right] + 2c. \quad (3.6)$$

Putting the two pieces together, the large- ℓ expansion of V reads

$$V_{\text{con}} = \sigma_s \ell + C + o(1), \quad \text{with} \quad C = \begin{cases} 2c - 2g\sqrt{s} \int_0^1 \frac{dv}{v^2} \left[1 + v^2 - e^{v^2} \left(1 - v^4 \frac{T^4}{T_c^4} \right)^{-\frac{1}{2}} \left(1 - v^4 e^{2(1-v^2)} \right)^{\frac{1}{2}} \right] & \text{if } T \leq T_c, \\ 2c - 2g\sqrt{s} \frac{T}{T_c} \int_0^1 \frac{dv}{v^2} \left[1 + v^2 - e^{v^2 \frac{T_c^2}{T^2}} \left(1 - v^4 \right)^{-\frac{1}{2}} \left(1 - v^4 e^{2\frac{T_c^2}{T^2}(1-v^2)} \right)^{\frac{1}{2}} \right] & \text{if } T \geq T_c. \end{cases} \quad (3.7)$$

To complete the picture, we now consider the small- ℓ behavior of the pseudopotential, which corresponds to the limit $\lambda \rightarrow 0$. Keeping only the leading terms in (3.1), we obtain

$$\ell = \frac{1}{2} \sqrt{\frac{\lambda}{s}} (B(\frac{3}{4}, \frac{1}{2}) + O(\lambda)), \quad V_{\text{con}} = \frac{1}{2} g \sqrt{\frac{s}{\lambda}} (B(-\frac{1}{4}, \frac{1}{2}) + O(\lambda)) + 2c, \quad (3.8)$$

where $B(a, b)$ is the beta function. From this, it immediately follows that

$$V_{\text{con}} = -\frac{\alpha}{\ell} + 2c + o(1), \quad \text{with} \quad \alpha = g \frac{(2\pi)^3}{\Gamma^4(\frac{1}{4})}. \quad (3.9)$$

Notably, to this order, V_{con} is independent of temperature and coincides with the heavy quark-antiquark potential at zero temperature [11, 13].

B. The disconnected configuration

The disconnected string configuration is shown on the right panel of Fig.1. The motivation for considering such a configuration comes from the construction of the heavy quark-antiquark potential in the presence of light quarks [9], where the disconnected configuration describes a pair of heavy-light mesons formed in the decay process $Q\bar{Q} \rightarrow Q\bar{q} + q\bar{Q}$. At zero quark chemical potential it consists of two identical parts. The areas swept out by the strings are obtained by parallel transporting them along the y -direction. The total action is given by

$$S = 2(S_{\text{NG}} + S_{\text{q}}|_{r=r_{\bar{q}}}), \quad (3.10)$$

where the boundary term describes a light quark (antiquark) attached to the string endpoint in the bulk.

We first extremize the action with respect to the string profiles. Since we are interested in the case in which x depends only on r , we choose the gauge $\xi^1 = y$ and $\xi^2 = r$. For the geometry (2.3), the Nambu-Goto action is then

$$S_{\text{NG}} = gY \int dr \frac{e^{sr^2}}{r^2} \sqrt{f^{-1} + (\partial_r x^i)^2}. \quad (3.11)$$

Here $Y = \int dy$. From this, it follows that $x^i = \text{const}$, which represents a straight string stretched along the r -axis, is a solution to the equations of motion.

As in [9], we consider a constant tachyon background T_0 . For the worldsheets shown in Fig.1, whose boundaries are lines in the y -direction, the boundary action written in the gauge $\tau = y$ takes the form

$$S_q = RT_0 Y \frac{e^{\frac{s}{2}r_q^2}}{r_q}. \quad (3.12)$$

One immediately recognizes this as the action of a point particle of mass T_0 at rest.

Combining these results, the corresponding pseudopotential $V_{\text{dis}} = S/Y$ is

$$V_{\text{dis}} = 2g \left(\int_0^{r_{\bar{q}}} \frac{dr}{r^2} \frac{e^{sr^2}}{\sqrt{f}} + n \frac{e^{\frac{s}{2}r_{\bar{q}}^2}}{r_{\bar{q}}} \right), \quad (3.13)$$

where $n = \frac{RT_0}{g}$. The integral diverges at $r = 0$ and therefore requires regularization. As in the case of the connected configuration [5], we implement this by imposing a cutoff ϵ on the lower limit of integration

$$\int_{\epsilon}^{r_{\bar{q}}} \frac{dr}{r^2} \frac{e^{sr^2}}{\sqrt{f}} = \frac{1}{\epsilon} - \frac{1}{r_{\bar{q}}} + \int_{\epsilon}^{r_{\bar{q}}} \frac{dr}{r^2} \left(\frac{e^{sr^2}}{\sqrt{f}} - 1 \right). \quad (3.14)$$

Subtracting the $\frac{1}{\epsilon}$ term and then taking $\epsilon \rightarrow 0$, we obtain the renormalized pseudopotential

$$V_{\text{dis}} = 2g \sqrt{\frac{s}{\bar{q}}} \left(\int_0^1 \frac{dv}{v^2} \left[e^{\bar{q}v^2} \left(1 - \bar{q}^2 v^4 \frac{T^4}{T_c^4} \right)^{-\frac{1}{2}} - 1 - v^2 \right] + n e^{\frac{\bar{q}}{2}} \right) + 2c, \quad (3.15)$$

where $\bar{q} = sr_{\bar{q}}^2$. Importantly, the normalization constant c is the same as in (3.1).

We still have to extremize the pseudopotential, or equivalently the action, with respect to $r_{\bar{q}}$. A simple calculation gives

$$e^{\frac{\bar{q}}{2}} + n(\bar{q} - 1) \sqrt{1 - \bar{q}^2 \frac{T^4}{T_c^4}} = 0. \quad (3.16)$$

This equation determines \bar{q} as a function of T . Its physical interpretation is as follows. It is the force balance equation at the light quark position. The two terms come from the gravitational force acting on the quark and the string tension at its position. Importantly, Eq.(3.16) makes sense only if the light quarks are closer to the boundary than the soft wall and horizon.

Thus, the pseudopotential associated with the disconnected configuration is given by the expression (3.15) evaluated on the solution to Eq.(3.16). Clearly, it is independent of the length ℓ .

C. Details for $SU(3)$ gauge theory

At this point, it makes sense to ask which configuration dominates in the sum (2.2). However, before answering this question, we need to specify the model parameters. In doing so, we use the same parameter set as in the case of the heavy quark-antiquark potential for $SU(3)$ gauge theory with two light quarks of equal mass [9]. First, the value of s is fixed from the slope of the Regge trajectory of $\rho(n)$ mesons in the soft wall model with the geometry (2.3), giving $s = 0.450 \text{ GeV}^2$ [14]. Then, using the expression for σ , we obtain $g = 0.176$ by fitting the string tension to its value in [15].⁷ Finally, the parameter n is adjusted to reproduce the lattice result for the string breaking distance ℓ_c [15]. With $\ell_c = 1.22 \text{ fm}$, this gives $n = 3.057$.

We are now in position to complete our discussion of the string configurations. Let us begin with the constant terms C and $2c$. The results are shown on the left panel of Fig.2. It is quite remarkable that the constant term C also

⁷ Note that fitting the coefficient α in (3.9) to the Lüsher value $\frac{\pi}{12}$ gives $g = 0.182$ that is quite satisfactory.

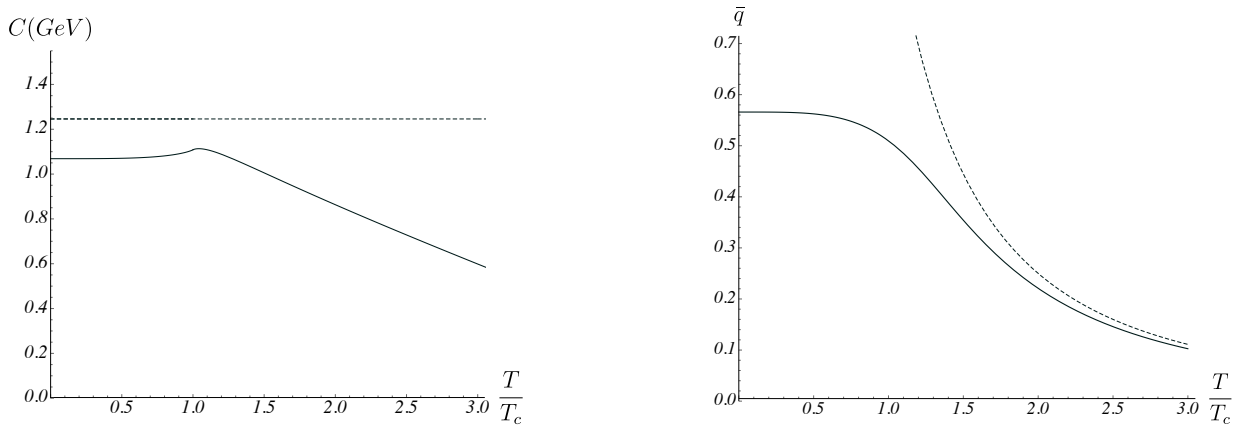


FIG. 2: Left: The constant terms C (solid) and $2c$ (dashed) as a function of temperature. We set $c = 0.623 \text{ GeV}$, here and below. Right: The solution of Eq.(3.16). The dashed curve corresponds to the horizon in units sr_h^2 . The soft wall is at 1 in these units.

exhibits the specific behavior, like the spatial string tension. Namely, at low temperatures, it remains nearly constant; it then begins to slightly grow near the transition point, reaches a maximum (visible as a small bump at $T = 1.04 T_c$), and finally decreases with temperature.⁸ It is worth noting that the inequality $C < 2c$ holds at all temperatures. In other words, the constant term in the large- ℓ expansion is smaller than that in the small- ℓ expansion.

The equation (3.16) can be solved numerically, with the result shown on the right panel of Fig.2. The solution also changes its behavior across the transition point, but it does so quite smoothly. Clearly, the light quarks are outside the horizon. This remains true at higher temperatures, where \bar{q} falls as $\sqrt{1 - n^{-2}} \frac{T^2}{T_c^2}$, while the horizon as $\frac{T_c^2}{T^2}$. With this solution, it is easy to find the temperature dependence of V_{dis} . For our parameter set, the result is presented on the left panel of Fig.3. We observe the specific behavior: the pseudopotential V_{dis} remains nearly constant at low temperatures, then smoothly transitions near the critical point, and exhibits noticeable growth at higher temperatures.

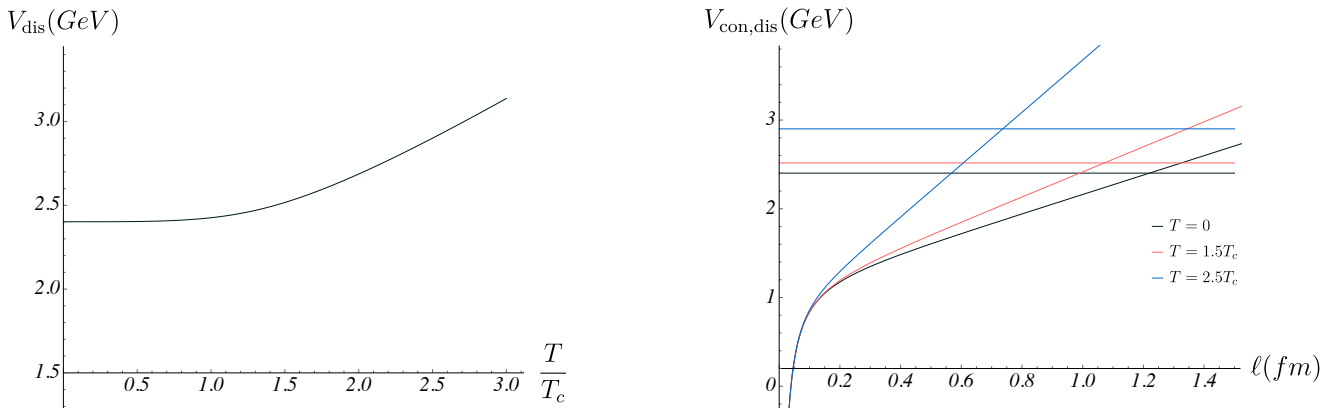


FIG. 3: Left: V_{dis} vs $\frac{T}{T_c}$. Right: V_{con} and V_{dis} vs ℓ at various temperatures.

This growth becomes linear for $T \gtrsim 5T_c$, where $V_{\text{dis}} = \frac{1}{2}g\sqrt{s}(B(1 - n^{-2}, -\frac{1}{4}, \frac{1}{2}) + \frac{4n^2}{\sqrt{n^2-1}})\frac{T}{T_c} + 2c + o(1)$. Here $B(z, a, b)$ denotes the incomplete beta function.

We are now in a position to proceed with the pseudopotentials V_{con} and V_{dis} . On the right panel of Fig.3, we plot both as a function of the length ℓ . V_{con} exhibits the temperature-dependent behavior at large lengths and the temperature-independent behavior at small lengths, in agreement with the lattice results [3]. Clearly, V_{con} dominates the pseudopotential V at small lengths, whereas V_{dis} dominates at large ones. Thus, the sum in Eq.(2.2) involves the

⁸ Note that $C = 2c - 2g\sqrt{s}\frac{T}{T_c} + O\left(\frac{T_c^2}{T^2}\right)$ at high temperatures.

two distinct string configurations. This implies that the pseudopotential is given by $V = \min\{V_{\text{con}}, V_{\text{dis}}\}$.

In practice, one particularly useful model, also used to determine the quark-antiquark potential [15], is that of [16]. It includes a mixing analysis based on a correlation matrix whose elements give rise to a model Hamiltonian. Adopting it for the problem in hand, we introduce

$$\mathcal{H}(\ell) = \begin{pmatrix} V_{\text{con}}(\ell) & \Theta \\ \Theta & V_{\text{dis}} \end{pmatrix}, \quad (3.17)$$

where the diagonal elements represent the contributions from the string configurations, and the off-diagonal element describes the strength of mixing between them. The pseudopotential is then the smaller eigenvalue of \mathcal{H} . Explicitly,⁹

$$V = \frac{1}{2}(V_{\text{con}} + V_{\text{dis}}) - \sqrt{\frac{1}{4}(V_{\text{con}} - V_{\text{dis}})^2 + \Theta^2}. \quad (3.18)$$

Although we have computed the diagonal elements of \mathcal{H} , calculating the off-diagonal element within the effective string model remains challenging. Because of this, it is impossible to precisely visualize the form of the pseudopotential. However, we can still gain valuable insight from our experiences with the heavy quark-antiquark potential, particularly regarding the approximate magnitude of the Θ value.¹⁰ This leads to the overall picture sketched in Figure 4 on the left. One important conclusion for what follows can be drawn from this result: the plots of V_{con} and V_{dis} intersect at

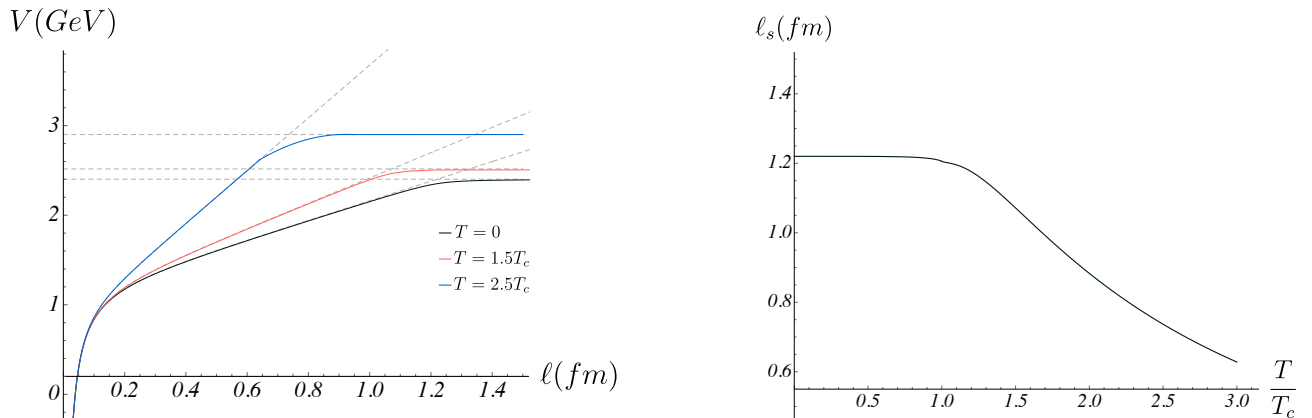


FIG. 4: Left: Sketched here is the pseudopotential at various temperatures. V_{con} and V_{dis} are shown in dashed lines. We set $\Theta = 50$ MeV at $T = 0$ and $T = 1.5T_c$. Right: The spatial string breaking distance as a function of temperature.

points near which V_{con} is approximately linear.

To quantitatively describe the flattening of the pseudopotential, we define the spatial string breaking distance ℓ_s by equating V_{con} and V_{dis}

$$V_{\text{con}}(\ell_s) = V_{\text{dis}}. \quad (3.19)$$

At zero temperature, this definition coincides with that of the string breaking distance introduced in [15] to characterize the heavy quark potential in the presence of light dynamical quarks. As a result, $\ell_s|_{T=0} = \ell_c$. Importantly, such defined ℓ_s is finite and scheme independent (i.e., independent of the normalization constant c). On the right panel in Fig.4, we plot ℓ_s against temperature. The spatial string breaking distance weakly decreases at low temperatures but continues to decrease noticeably across the transition point. Thus, it also shows the specific behavior. By contrast, the string breaking distance ℓ_c increases weakly near zero temperature but rises more noticeably as temperature approaches the critical value [9], becoming meaningless beyond the transition point.

⁹ The larger eigenvalue gives the pseudopotential V_1 (the subleading exponent in (1.1)) corresponding to the excited state.

¹⁰ For instance, one can assume that Θ is approximately constant, with a value around 50 MeV, as found on the lattice at zero temperature [15].

The Eq.(3.19) can be solved approximately if V_{con} is nearly linear. In this case, with the help of the asymptotic expansion (3.7), we find that

$$\ell_s \approx \frac{1}{\sigma_s} (V_{\text{dis}} - C). \quad (3.20)$$

In fact, this is a rather accurate approximation. In the temperature range $0 \leq T \leq 3T_c$, the difference between the solution of Eq.(3.19) and its approximation (3.20) appears only in the third digit after the decimal point. It is worth noting that the specific temperature behavior of the spatial string breaking distance follows directly from this formula. Indeed, all the terms on the right hand side exhibit the specific behavior across the transition point. Another conclusion is that ℓ_s scales as $\frac{1}{T}$ at very high temperatures.

IV. CONCLUDING COMMENTS

In the context of the spatial Wilson loops, we considered string breaking to gain insight into the nonperturbative features of QCD with two light flavors. No phenomenological or lattice predictions yet exist in this context, but the effective string model at our disposal enables some predictions. In particular, we estimated the spatial string breaking distance for $SU(3)$ gauge theory in the temperature range $0 - 3T_c$.

The use of the effective string model at high temperatures requires a caveat. The temperature dependence of the spatial string tension agrees with the lattice data only for temperatures below $2.5 - 3T_c$, at least for pure gauge theories [5]. The similar holds for the Coulomb coefficient α defined in (3.9) which begins to decrease at higher temperatures and eventually approaches the Lüscher value $\frac{\pi}{24}$.¹¹

We treated the off-diagonal element Θ of the model Hamiltonian as a free parameter. It would be of further interest to develop a string theory technique that enables its direct computation. Meanwhile, it would also be interesting to compute the model Hamiltonian \mathcal{H} using lattice QCD or the 3-dimensional effective field theory.

Acknowledgments

We would like to thank Michele Caselle, Peter Petreczky and Peter Weisz for useful communications and for comments on the manuscript. We also thank Dima Levkov for hospitality at ITMP, where part of this work was completed.

-
- [1] Y. Aoki, G. Endrodi, Z. Fodor, S.D. Katz, and K.K. Szabo, *Nature (London)* **443**, 675 (2006).
[2] C. Borgs, *Nucl.Phys.* **B261**, 455 (1985); E. Manousakis and J. Polonyi, *Phys.Rev.Lett.* **58**, 847 (1987).
[3] The following is an incomplete list:
G. Bali, J. Fingberg, U.M. Heller, F. Karsch, and K. Schilling, *Phys.Rev.Lett.* **71**, 3059 (1993);
M. Caselle and A. D'Adda, *Nucl.Phys.B* **427**, 273 (1994);
F. Karsch, E. Laermann, and M. Lütgemeier, *Phys.Lett.B* **346** (1995) 94;
M. Cheng *et al.*, *Phys.Rev.D* **78**, 034506 (2008);
D. Bala, O. Kaczmarek, P. Petreczky, S. Sharma, and S. Tah, *Phys.Rev.Lett.* **135**, 012301 (2025).
[4] J. Casalderrey-Solana, H. Liu, D. Mateos, K. Rajagopal, and U.A. Wiedemann, *Gauge/String Duality, Hot QCD and Heavy Ion Collisions*, Cambridge University Press, 2014.
[5] O. Andreev and V.I. Zakharov, *Phys.Lett.B* **645** (2007) 437; O. Andreev, *Phys.Lett.B* **659** (2008) 416.
[6] C.D. White, *Phys.Lett.B* **652**, 79 (2007).
[7] O. Andreev and V.I. Zakharov, *Phys.Rev.D* **76**, 047705 (2007).
[8] J. Erlich, E. Katz, D.T. Son, and M.A. Stephanov, *Phys.Rev.Lett.* **95**, 261602 (2005).
[9] O. Andreev, *Phys.Lett.B* **804**, 135406 (2020); *Phys.Rev.D* **101**, 106003 (2020).
[10] O. Andreev, *Phys.Rev.D* **87**, 065006 (2013).
[11] J. Maldacena, *Phys.Rev.Lett.* **80**, 4859 (1998).
[12] I.Ya. Aref'eva, A. Hajilou, K. Rannu, and P. Slepov, *Spatial Wilson Loops and Energy Loss for Heavy Quarks in Magnetized HQCD Model*, arXiv:2601.09611 [hep-th].

¹¹ See, for example, the last reference in [3].

- [13] O. Andreev and V.I. Zakharov, Phys.Rev.D **74**, 025023 (2006).
- [14] O. Andreev, Phys.Rev.D **73**, 107901 (2006).
- [15] J. Bulava, B. Hörz, F. Knechtli, V. Koch, G. Moir, C. Morningstar, and M. Peardon, Phys.Lett.B **793**, 493 (2019).
- [16] I.T. Drummond, Phys.Lett.B **434**, 92 (1998).